

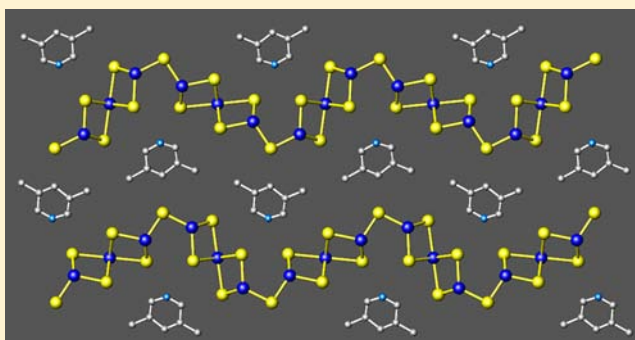
[C₇H₁₀N][In₃Se₅]: A Layered Selenide with Two Indium Coordination Environments

Sarah J. Ewing, Anthony V. Powell, and Paz Vaqueiro*

Department of Chemistry, Heriot-Watt University, Edinburgh EH14 4AS, U.K.

S Supporting Information

ABSTRACT: A new layered indium selenide, [C₇H₁₀N][In₃Se₅] (**1**), has been prepared solvothermally using 3,5-dimethylpyridine as a solvent and structure-directing agent. This material, which was characterized by single-crystal and powder X-ray diffraction, thermogravimetric analysis, UV–vis diffuse-reflectance spectroscopy, IR spectroscopy, and elemental analysis, crystallizes in the monoclinic space group *P*2₁/*c* [*a* = 3.9990(4) Å, *b* = 16.7858(15) Å, *c* = 23.930(2) Å, and β = 94.728(4)°]. The crystal structure of **1** contains anionic layers of stoichiometry [In₃Se₅][−] in which indium atoms with octahedral and tetrahedral coordination coexist. The [In₃Se₅][−] layers are interspaced by monoprotonated 3,5-dimethylpyridinium cations. A closely related material, [C₇H₁₀N][In₃Se₅] (**2**), was obtained when using 2,6-dimethylpyridine instead of 3,5-dimethylpyridine.



INTRODUCTION

Solvothermally prepared metal chalcogenides are a focus of research activity because of their range of potential applications, which include catalysis,¹ selective ion exchange,² and molecule-discriminating sensors.³ Structure-directed synthesis is widely used to prepare such metal chalcogenides, and previous research efforts have resulted in many structurally diverse materials containing main-group elements from groups 13 (Ga and In),⁴ 14 (Ge and Sn),⁵ and 15 (Sb and As).^{5,6} However, most of the work to date has centered on sulfides, and by comparison, only a relatively small number of selenides and tellurides have been reported.

For solvothermally prepared group 13 chalcogenides, the primary building block that has been most frequently observed is the MQ₄ tetrahedron (M = Ga, In; Q = S, Se, Te). These tetrahedral building units can be linked by their corners or edges, and this leads to a variety of different secondary building blocks and arrangements. While the structural chemistry of group 13 sulfides is dominated by supertetrahedral clusters,⁴ which are formed by corner linkage of MQ₄^{5−} tetrahedra, only a small number of selenides and tellurides containing such clusters have been reported to date. For indium, this includes the layered [In(en)₃][In₅Te₉(en)₂]·0.5en, which is a polar, chiral material with nonlinear optical behavior,⁷ the super-tetrahedra-based double-diamond lattice found in the [In₁₀Se₁₈]^{6−} open framework,⁸ and the single-diamond lattice of the [In₄Se₅]^{4−} structure.⁹ Indium selenides and tellurides show a greater degree of structural complexity than the analogous sulfides. For example, edge sharing of InQ₄^{5−} tetrahedra (Q = S, Se, Te) can result in the formation of one-dimensional [InQ₂][−] chains,¹⁰ and for the heavier

chalcogenides, replacement of Q^{2−} with polychalcogenide Q_n^{2−} anions in the [InQ₂][−] chains leads to the formation of a family of one-dimensional chains, as exemplified by [M(en)₃][In₂Te₂(Te₂)₂] (M = Fe, Zn),¹¹ [C₆H₁₆N₂][In₂Se₃(Se₂)],¹² and other related compounds.¹³ Complex cationic chains, in which four- and five-coordinate indium atoms coexist, have been found in [{In(dien)}₂(InTe₄)]·Cl.¹⁴ Linkage of InSe₄^{5−} tetrahedra can also lead to three-dimensional frameworks. This is exemplified by [C₇H₁₀N][In₉Se₁₄], which contains edge- and corner-sharing InSe₄^{5−} tetrahedra and possesses one-dimensional channels with a diameter of ca. 6 Å,¹⁵ and the structure of [In₃₃Q₅₆]^{13−} (Q = S, Se, Te),¹⁶ which consists of cross-linked helical chains of corner-sharing InQ₄ tetrahedra. Corner linking of InSe₄^{5−} tetrahedra is also found in the microporous structure of [NH₄]₄[In₁₂Se₂₀], in which nonanuclear indium clusters serve as secondary building units.¹⁷

Here, we report the synthesis, crystal structure, and optical properties of a unique layered indium selenide, prepared solvothermally using dimethylpyridine as a solvent and structure-directing agent. In contrast with previously reported structures,^{8,9,12,15–17} which are based on InSe₄^{5−} tetrahedral building blocks, the material described here contains indium atoms coordinated by selenium with two distinct coordination environments, octahedral and tetrahedral. To the best of our knowledge, this is the first occurrence of an InSe₆^{9−} octahedral building block in a solvothermally prepared indium selenide. The coexistence of tetrahedral and octahedral units in a

Received: April 27, 2012

Published: June 20, 2012

solvothermally prepared indium sulfide was reported very recently for the first time.¹⁸

EXPERIMENTAL SECTION

Synthesis. For the preparation of $[\text{C}_7\text{H}_{10}\text{N}][\text{In}_3\text{Se}_5]$ (**1**), indium powder (Alfa Aesar, 99+%, 0.1676 g, 1.46 mmol), selenium powder (Aldrich, 99.5%, 1.958 g, 2.48 mmol), and 3,5-dimethylpyridine (Aldrich, 98+%, 7.5 mL, 66 mmol) were loaded individually into a 23 mL Teflon-lined stainless steel autoclave, giving an approximate molar composition In/Se/ $\text{C}_7\text{H}_9\text{N}$ of 1.46:2.5:66. After the reaction mixture was stirred for approximately 10 min, the vessel was closed, heated at 185 °C for 10 days, and then cooled to room temperature at a cooling rate of 0.2 °C min^{-1} . The solid product was filtered and washed with methylated spirits and acetone before drying in air at room temperature. Under these reaction conditions, the product consisted of a large amount of yellow needles, together with a small amount of brown powder and red needles. The yellow needles were later identified by single-crystal X-ray diffraction as the title compound **1**. Analysis of powder X-ray diffraction data indicates that the brown powder is In_2Se_3 , while the red needles were identified by single-crystal X-ray diffraction as the previously reported selenide $[\text{C}_7\text{H}_{10}\text{N}][\text{In}_9\text{Se}_{14}]$.¹⁵

Using 2,6-dimethylpyridine (Aldrich, 98%), with the same molar ratios but a reaction temperature of 200 °C for 10 days, a small amount of yellow needles, together with a black powder, were produced. These yellow needles were identified by single-crystal X-ray diffraction as $[\text{C}_7\text{H}_{10}\text{N}][\text{In}_3\text{Se}_5]$ (**2**). This reaction only produces a very small amount of **2**, which prevented reliable analytical data for this compound being obtained.

Characterization. Powder X-ray diffraction data were collected using a Bruker D8 Advance powder diffractometer, operating with germanium monochromated $\text{Cu K}\alpha_1$ radiation ($\lambda = 1.5406 \text{ \AA}$) fitted with a Bruker LynxEye linear detector. Data were collected, on a ground portion of the reaction product, over the angular range $5 \leq 2\theta/\text{deg} \leq 85$ with a step size of 0.009° . Lattice parameters were determined using TOPAS.¹⁹ Elemental analysis on handpicked crystals of **1** was carried out on an Exeter CE-440 elemental analyzer. Thermogravimetric analysis was performed using a DuPont Instruments 951 thermal analyzer. Approximately 10 mg of finely ground crystals was heated under a flow of O_2 over the temperature range $30 \leq T/^\circ\text{C} \leq 1000$ using a heating rate of 2°C min^{-1} . Diffuse-reflectance measurements were performed using a Perkin-Elmer Lambda 35 UV-vis spectrometer. BaSO_4 powder was used as a reference (100% reflectance), and absorption data were calculated from the Kubelka–Munk function.²⁰ The IR spectrum of **1** was obtained using a 100 ATR spectrophotometer, on a ground sample of handpicked crystals.

Single-crystal X-ray diffraction was carried out at 293 K using a Bruker X8 APEX diffractometer ($\text{Mo K}\alpha$; $\lambda = 0.71073 \text{ \AA}$).²¹ Crystals were mounted with a cyanoacrylate adhesive onto a glass fiber. Intensity data were collected at 30 s intervals per rotation for **1** and at 40 s per rotation for **2**. Structure **1** was solved by direct methods using the program SIR92,²² which located the indium and selenium atoms. Structure **2** was solved using the program Superflip.²³ Subsequent Fourier calculations and least-squares refinements on F were carried out using the CRYSTALS program.²⁴ The carbon and nitrogen atoms of the amine were located in the difference Fourier maps. Hydrogen atoms were placed geometrically after each cycle of refinement, but their positions were not refined. For **1**, after location of all of the atoms, R_w remained high (>0.27), and examination of the data suggested that the crystal could be twinned. The program ROTAX²⁵ was used to identify a possible twin law. Twinning could be defined by the following matrix:

$$\begin{pmatrix} 1 & 0 & 0 \\ 0 & -1 & 0 \\ -1 & 0 & -1 \end{pmatrix}$$

Twin fractions refined to 0.523(2) and 0.477(2), respectively, and gave a significantly lower final residual, R_w , of 0.0465. Selected crystallographic data for **1** and **2** are presented in Table 1.

Table 1. Selected Crystallographic Data for $[\text{C}_7\text{H}_{10}\text{N}][\text{In}_3\text{Se}_5]$

	1	2
M_r	847.42	847.42
crystal size (mm)	$0.03 \times 0.03 \times 0.10$	$0.01 \times 0.01 \times 0.06$
crystal habit	yellow needles	yellow needles
crystal system	monoclinic	orthorhombic
space group	$P2_1/c$	$P22_12_1$
a (Å)	3.9990(4)	4.0034(4)
b (Å)	16.7858(15)	16.9343(14)
c (Å)	23.930(2)	23.2483(19)
β (deg.)	94.728(4)	
unit cell volume (Å ³)	1600.9(3)	1576.1(2)
Z	4	4
ρ_{cal} (g cm^{-3})	3.516	3.571
θ_{max} (deg.)	26.4	27.1
radiation	$\text{Mo K}\alpha$	$\text{Mo K}\alpha$
temperature (K)	293	293
R_{merg}	0.0619	0.084
unique data	3231	3395
obsd. data [$I > 3\sigma(I)$]	1659	2895
no. of param. refined	109	107
residual electron density max. (e Å ⁻³)	2.04	4.63
residual electron density min. (e Å ⁻³)	-2.03	-2.73
R	0.0578	0.0723
R_w	0.0465	0.0819

RESULTS AND DISCUSSION

Powder X-ray diffraction data (Supporting Information) of the bulk reaction product show that **1** is the main product under the stated conditions. The lattice parameters determined for **1** using powder diffraction data [$a = 3.994(5) \text{ \AA}$, $b = 16.770(4) \text{ \AA}$, $c = 23.96(1) \text{ \AA}$, and $\beta = 95.27(1)^\circ$] are in reasonable agreement with those determined by single-crystal X-ray diffraction (Table 1). **1** was initially identified as a minority phase in the product of the reaction carried out at 200 °C, which contained mainly In_2Se_3 and the previously reported $[\text{C}_7\text{H}_{10}\text{N}][\text{In}_9\text{Se}_{14}]$.¹⁵ A range of temperatures and molar ratios were explored to produce a single-phase product. Upon reduction of the temperature to 185 °C, a higher yield of the desired phase was obtained, with only a very small amount of In_2Se_3 and $[\text{C}_7\text{H}_{10}\text{N}][\text{In}_9\text{Se}_{14}]$. Compound **1** can be obtained within the temperature range 170–200 °C. Small amounts of a closely related compound, **2**, were obtained using the 2,6-dimethylpyridine isomer. Powder diffraction data for **2**, which are shown in the Supporting Information, indicate that the product of this reaction consists mainly of **2** and an unidentified phase. Attempts to optimize this reaction, to increase both the yield and size of the crystals of **2**, have been unsuccessful.

The local coordination diagram and atom labeling scheme for **1** are shown in Figure 1. The crystal structure of this material consists of anionic $[\text{In}_3\text{Se}_5]^-$ layers, separated by monoprotonated 3,5-dimethylpyridinium cations. There are four crystallographically independent indium atoms, which adopt two distinct coordination geometries. While In(1) and In(4) are octahedrally coordinated by six selenium atoms, In(2)

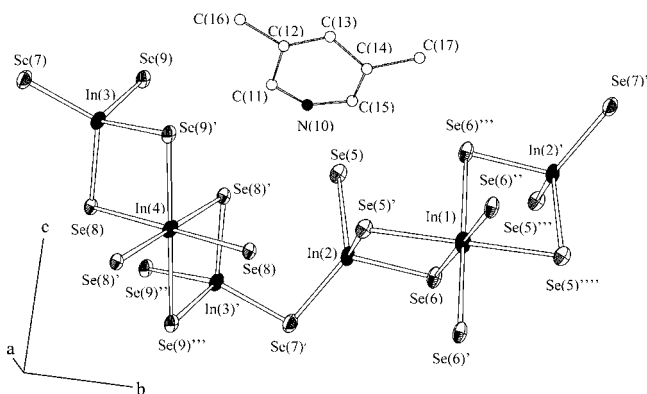


Figure 1. Local coordination diagram of non-hydrogen atoms for **1** showing the atom labeling scheme and ellipsoids at 50% probability.

and In(3) are surrounded by four selenium atoms in a tetrahedral geometry. Both the InSe_6 octahedra and the InSe_4 tetrahedra are slightly distorted (Table 2). For the two

Table 2. Selected Bond Lengths (Å) for **1**^a

bond	length (Å)
In(1)–Se(5)	2.892(2)
In(1)–Se(5) ^a	2.892(2)
In(1)–Se(6)	2.734(3)
In(1)–Se(6) ^a	2.734(3)
In(1)–Se(6) ^{b,c}	2.787(3) × 2
In(2)–Se(5)	2.610(3)
In(2)–Se(5) ^d	2.593(3)
In(2)–Se(6)	2.594(3)
In(2)–Se(7)	2.512(3)
In(3)–Se(7)	2.510(3)
In(3)–Se(8)	2.599(2)
In(3)–Se(9)	2.606(3)
In(3)–Se(9) ^b	2.603(3)
In(4)–Se(8)	2.772(3)
In(4)–Se(8) ^{b,e}	2.732(3) × 2
In(4)–Se(8) ^f	2.772(3)
In(4)–Se(9) ^{b,e}	2.8767(19) × 2

^aSymmetry transformations used to generate equivalent atoms: a, $1 - x, -y, 1 - z$; b, $1 + x, y, z$; c, $-x, -y, 1 - z$; d, $-1 + x, y, z$; e, $-x, 1 - y, 1 - z$; f, $1 - x, 1 - y, 1 - z$.

octahedrally coordinated indium atoms, the axial distances, which range between 2.892(2) and 2.8767(19) Å, are slightly longer than the equatorial distances [2.732(3)–2.787(3) Å]. All of the In–Se distances are within the range previously reported for octahedrally coordinated indium.²⁶ For the InSe_4 tetrahedra, the In–Se distances are shorter than those for octahedrally coordinated indium and lie within the range 2.510(3)–2.610(3) Å. This is consistent with previous findings for other indium selenides containing tetrahedrally coordinated indium.^{12,15} With the exception of Se(7), which is only bicoordinated, the other four crystallographically independent selenium atoms are coordinated to three indium atoms.

In the crystal structure of **1**, each In(1)Se_6 octahedron shares two opposite edges with two neighboring In(1)Se_6 octahedra, forming a one-dimensional chain of stoichiometry $[\text{InSe}_4]^{5-}$ (Figure 2). Similarly, In(4)Se_6 octahedra are linked by sharing edges into one-dimensional $[\text{InSe}_4]^{5-}$ chains. Each InSe_4 tetrahedron shares two corners with two neighboring InSe_4

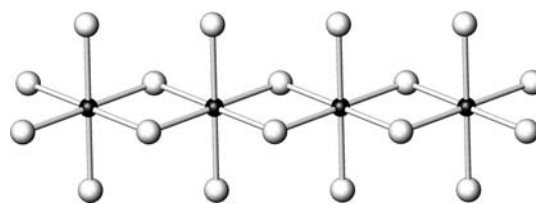


Figure 2. One-dimensional $[\text{InSe}_4]^{5-}$ chains, formed by edge-sharing InSe_6^{9-} octahedra. Key: indium, large solid circles; selenium, large open circles.

tetrahedra (Figure 3), generating two crystallographically distinct $[\text{InSe}_3]^{3-}$ chains, which contain exclusively In(2) or

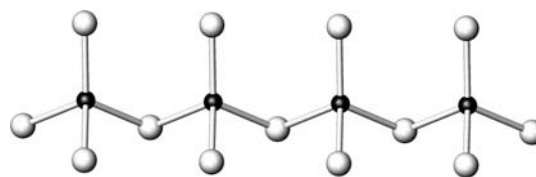


Figure 3. One-dimensional $[\text{InSe}_3]^{3-}$ chains, created via corner sharing of InSe_4^{5-} tetrahedra. Key: indium, large solid circles; selenium, large open circles.

In(3) atoms. One-dimensional ribbons, of stoichiometry $[\text{In}_3\text{Se}_6]^{3-}$, are formed by linking one octahedral $[\text{InSe}_4]^{5-}$ chain with two tetrahedral $[\text{InSe}_3]^{3-}$ chains (Figure 4). In these

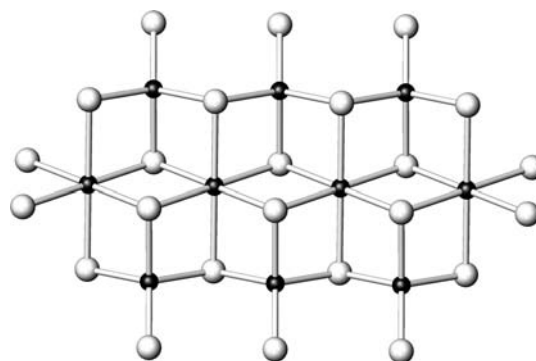


Figure 4. One-dimensional ribbon of stoichiometry $[\text{In}_3\text{Se}_6]^{3-}$, created from the linkage of one octahedral $[\text{InSe}_4]^{5-}$ chain with two tetrahedral $[\text{InSe}_3]^{3-}$ chains. Key: indium, large solid circles; selenium, large open circles.

ribbons, each tetrahedron shares two adjacent edges with two neighboring octahedra. There are two crystallographically distinct $[\text{In}_3\text{Se}_6]^{3-}$ ribbons, one of which contains In(1) and In(2), while the second one contains In(3) and In(4). These ribbons, which are directed along [100], are linked into zigzag layers, of stoichiometry $[\text{In}_3\text{Se}_5]^{-}$, by sharing the remaining vertex [Se(7)] of each tetrahedron with a neighboring ribbon (Figure 5a). These $[\text{In}_3\text{Se}_5]^{-}$ layers are also oriented parallel to the [100] direction.

In the crystal structure of **1**, the anionic $[\text{In}_3\text{Se}_5]^{-}$ layers are stacked along the [001] direction and are separated by ca. 8 Å. Monoprotonated 3,5-dimethylpyridinium cations are located in the void space between layers (Figure 5a). The nitrogen atom from each organic cation is oriented toward two selenium atoms, Se(5) and Se(8), of an $[\text{In}_3\text{Se}_5]^{-}$ layer. The N–Se distances are 3.65(2) and 3.49(2) Å, respectively. These are of a magnitude comparable to those of N–H⋯Se interactions

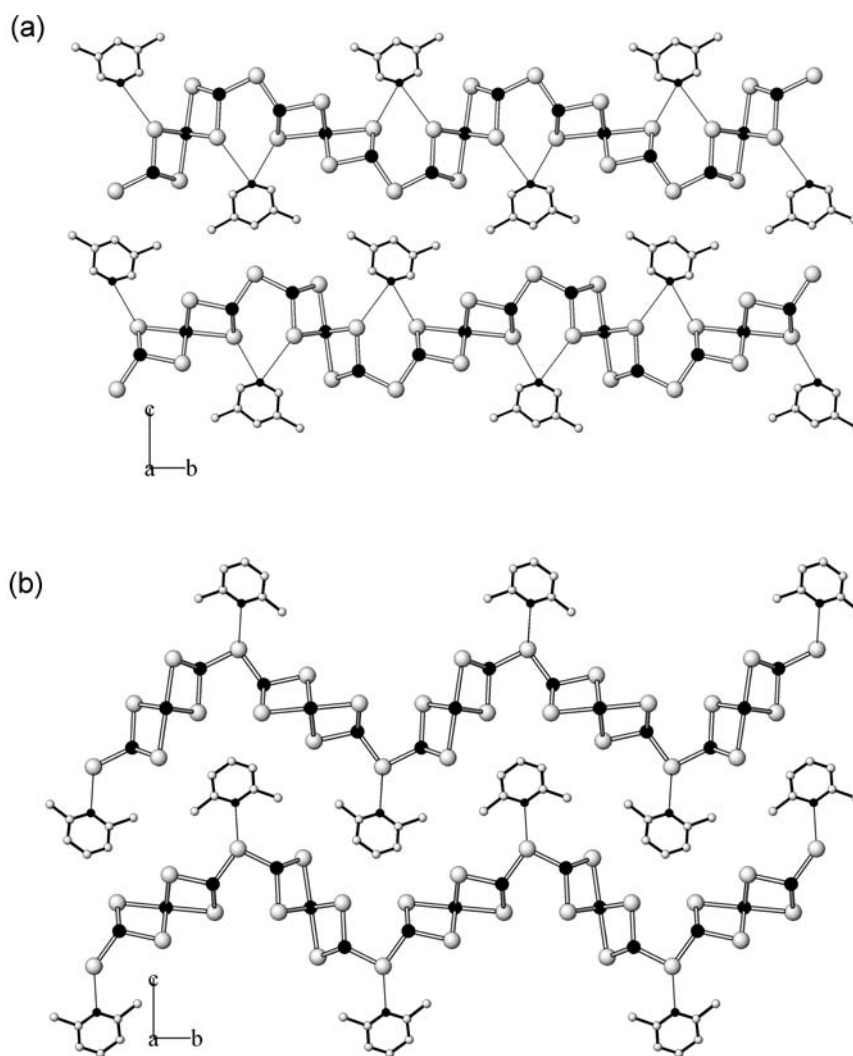


Figure 5. View of (a) **1** and (b) **2** along the [100] direction, showing the $[\text{In}_3\text{Se}_5]^{3-}$ layers, created from the linkage of one-dimensional $[\text{In}_3\text{Se}_6]^{3-}$ ribbons. The $[\text{In}_3\text{Se}_5]^{3-}$ layers are separated by monoprotonated dimethylpyridinium cations, and lines show the short Se–N distances. Key: indium, large solid circles; selenium, large open circles; carbon, small open circles; nitrogen, small solid circles.

described in the literature,¹² suggesting the presence of hydrogen-bonding interactions between the organic cations and the anionic layers. The crystal structure of **2** contains the same $[\text{In}_3\text{Se}_5]^{3-}$ layers, which are stacked along the [001] direction and separated by 2,6-dimethylpyridinium cations (Figure 5b). The hydrogen-bonding interactions are, however, different from those found in **1** because of the different positions of the amine functional group. While the location of the organic cations and the orientation of the methyl groups hardly change, in **2** each nitrogen atom is oriented toward two crystallographically equivalent Se(7) atoms, with N–Se distances of 3.35(2) and 3.37(2) Å.

The Fourier transform infrared (FT-IR) spectrum (Supporting Information) of **1** is consistent with the presence of aromatic and amine functional groups. A broad peak at $\sim 3058\text{ cm}^{-1}$ can be assigned to N–H stretching vibrations. Lower intensity peaks at $\sim 3000\text{ cm}^{-1}$ can be attributed to C–H stretching vibrations, while those within the region of $1600\text{--}1400\text{ cm}^{-1}$ are characteristic of aromatic compounds.²⁷ Elemental analysis (%) using handpicked crystals gave the following: C, 9.77; H, 0.83; N, 1.13, which agrees well with the values calculated from the crystallographically determined formula $[\text{C}_7\text{H}_{10}\text{N}][\text{In}_3\text{Se}_5]$ (C, 9.91; H, 1.19; N, 1.65).

Thermogravimetric analysis indicates that, under an oxygen atmosphere, **1** is stable to ca. $200\text{ }^\circ\text{C}$ (Supporting Information). The overall weight loss (46.6%) is in reasonable agreement with the calculated weight loss (50.86%) for decomposition of the title compound into In_2O_3 . The identity of the decomposition product, which is a white powder, was confirmed as In_2O_3 by powder X-ray diffraction (Supporting Information).

The optical absorption spectrum of **1** is shown in Figure 6. The optical band gap, which was estimated from the absorption edge, has a value of 2.48(4) eV at room temperature, consistent with the yellow color of the crystals. When compared to $[\text{C}_7\text{H}_{10}\text{N}][\text{In}_9\text{Se}_{14}]$,¹⁵ which was prepared using the same amine but at a higher temperature ($200\text{ }^\circ\text{C}$) than the title compound ($185\text{ }^\circ\text{C}$), $[\text{C}_7\text{H}_{10}\text{N}][\text{In}_9\text{Se}_{14}]$ has a smaller optical band gap [1.91(6) eV] than **1**. Analysis of a wide range of antimony sulfides has led to identification of a correlation between the optical band gap and the framework density of the main-group metal centers.²⁸ Generally, it was noted that increasing the framework density leads to a decrease of the band gap of the material. Similar behavior is observed here. The layered **1** is less dense than the three-dimensional framework of $[\text{C}_7\text{H}_{10}\text{N}][\text{In}_9\text{Se}_{14}]$ and consequently exhibits a larger band

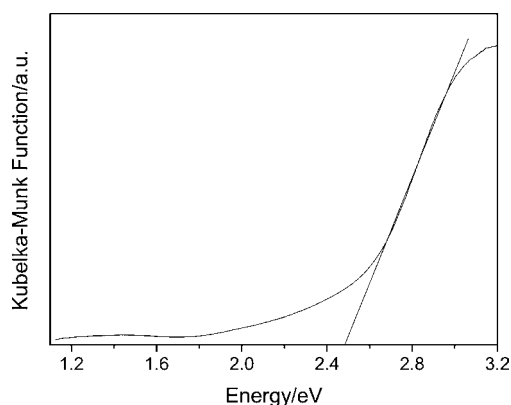


Figure 6. Diffuse-reflectance data for **1**. The straight line shows extrapolation from the high-energy end of the absorption edge used to determine the band gap.

gap. This may be related to the weakening of interactions between the indium and selenium atomic orbitals with decreasing framework density, with the result that the tail on the low-binding-energy side of the valence band is contracted.²⁸

Previous work on the solvothermal synthesis of indium selenides has resulted in materials containing InSe_4^{5-} primary building blocks.^{8,9,10b,c,12,13a,15–17} This contrasts markedly with the structural chemistry of indium selenides prepared by high-temperature methods, for which a far greater degree of structural diversity has been reported. For instance, in In_2Se_3 , which crystallizes in three polymorphic forms, indium can be found in tetrahedral, octahedral, and trigonal-bipyramidal coordination,²⁹ while in the structure of other binary selenides, such as InSe ³⁰ or In_4Se_3 ,³¹ In–In bonds have been identified. The results presented here demonstrate that a similar degree of complexity may be achievable in indium selenides prepared by solvothermal synthesis. Moreover, we can draw some parallels between the secondary building blocks found in the title compound and those previously reported for condensed phases of ternary and quaternary indium selenides. In particular, the linear $[\text{InSe}_4]^{5-}$ chain of edge-sharing octahedra (Figure 2) has been previously observed in ternary metal chalcogenides of the type Ln_3InQ_6 (where Ln = Sm, Gd, Pr and Q = S, Se),^{26b–d} while coexistence of tetrahedrally and octahedrally coordinated indium has been found in the related ternary condensed phase La_3InS_6 ³² as well as in the family of quaternary selenides $\text{Ca}_4(\text{Ln})_2\text{In}_4\text{Se}_{13}$ (Ln = La, Nd, Sm, Gd).^{26a} $[\text{In}_3\text{Se}_6]^{3-}$ ribbons, similar to those reported for the title compound (Figure 4), have been found in TlIn_5Se_8 .³³ The latter material, however, crystallizes in a different structural type, in which alternating $[\text{In}_3\text{Se}_6]^{3-}$ and $[\text{In}_2\text{Se}_4]^{2-}$ ribbons are linked into layers. Long In–Se bonds ($>3 \text{ \AA}$) join these layers in a three-dimensional structure, which contains Tl^+ cations in channels parallel to the *b* axis. Although there are known sulfides and selenides with a 3:5 molar ratio of indium to chalcogen found in the title compound, these materials adopt entirely different structural types. This includes the ternary sulfides MIn_3S_5 (M = Rb, Cs),³⁴ with a three-dimensional structure consisting of layers of edge-sharing octahedra linked by chains of corner-sharing tetrahedra, and CuIn_3Se_5 , which adopts a structure related to that of chalcopyrite.³⁵ To the best of our knowledge, the crystal structure described here constitutes a new structural type.

In conclusion, the results presented here demonstrate that selenides containing non tetrahedrally coordinated indium can be obtained under solvothermal conditions, and this is expected

to lead to a higher degree of structural diversity than was previously envisaged. In addition, identification of the $[\text{In}_3\text{Se}_6]^{3-}$ ribbons in the layers of **1** and **2**, as well as in the previously reported TlIn_5Se_8 ,³³ suggests that this ribbon may be a relatively common building block in indium selenides. Linkage of such $[\text{In}_3\text{Se}_6]^{3-}$ ribbons to other building units may give access to a range of new two- or three-dimensional structures.

■ ASSOCIATED CONTENT

Supporting Information

CIF files for the crystal structures and powder X-ray diffraction data for **1** and **2**, tables of atomic coordinates, bond angles, and hydrogen bonds, and TGA and FT-IR data for **1**. This material is available free of charge via the Internet at <http://pubs.acs.org>.

■ AUTHOR INFORMATION

Corresponding Author

*E-mail: chepv@hw.ac.uk. Fax: +44(0)131 451 3180.

Notes

The authors declare no competing financial interest.

■ ACKNOWLEDGMENTS

The authors thank UK EPSRC for financial support and Christina Graham for elemental analysis.

■ REFERENCES

- (1) Zheng, N.; Bu, X.; Vu, H.; Feng, P. *Angew. Chem., Int. Ed.* **2005**, *44*, 5299–5303.
- (2) Manos, M. J.; Chrissafis, K.; Kanatzidis, M. G. *J. Am. Chem. Soc.* **2006**, *128*, 8875–8883.
- (3) Ozin, G. A. *Supramol. Chem.* **1995**, *6*, 125–134.
- (4) (a) Feng, P.; Bu, X.; Zheng, N. *Acc. Chem. Res.* **2005**, *38*, 293–303. (b) Bu, X.; Zheng, N.; Feng, P. *Chem.—Eur. J.* **2004**, *10*, 3356–3362.
- (5) (a) Dehnen, S.; Melullis, M. *Coord. Chem. Rev.* **2007**, *251*, 1259–1280. (b) Sheldrick, W. S. *J. Chem. Soc., Dalton Trans.* **2000**, 3041–3052. (c) Sheldrick, W. S.; Wachold, M. *Coord. Chem. Rev.* **1998**, *176*, 211–322.
- (6) Powell, A. V. *Int. J. Nanotechnol.* **2011**, *8*, 783–794.
- (7) Zhang, Q. C.; Chung, I.; Jang, J. L.; Ketterson, J. B.; Kanatzidis, M. G. *Chem. Mater.* **2009**, *21*, 12–14.
- (8) Wang, C.; Bu, X.; Zheng, N.; Feng, P. *Chem. Commun.* **2002**, 1344–1345.
- (9) Zheng, N.; Bu, X.; Feng, P. *Nature* **2003**, *426*, 428–432.
- (10) (a) Vaqueiro, P. *J. Solid State Chem.* **2006**, *179*, 302–307. (b) Zhou, J.; Bian, G. Q.; Zhang, Y.; Zhu, Q. Y.; Li, C. Y.; Dai, J. *Inorg. Chem.* **2007**, *46*, 6347–6352. (c) Zhou, J.; Zhang, Y.; Bian, G. Q.; Zhu, Q. Y.; Li, C. Y.; Dai, J. *Cryst. Growth. Des.* **2007**, *7*, 1889–1892.
- (11) Li, J.; Chen, Z.; Emge, T. J.; Proserpio, D. M. *Inorg. Chem.* **1997**, *36*, 1437–1442.
- (12) Ewing, S. J.; Powell, A. V.; Vaqueiro, P. *J. Solid State Chem.* **2011**, *184*, 1800–1804.
- (13) (a) Xiong, W. W.; Li, J.-R.; Feng, M.-L.; Huang, X.-Y. *CrystEngComm* **2011**, *13*, 6206–6311. (b) Yao, H. G.; Ji, M.; Ji, H. S.; An, Y. L. *Z. Anorg. Allg. Chem.* **2012**, *638*, 683–687. (c) Zhang, X.; Lei, Z. X.; Luo, W.; Mu, W. Q.; Zhang, X.; Zhu, Q. Y.; Dai, J. *Inorg. Chem.* **2011**, *50*, 10872–10877.
- (14) Li, C. Y.; Chen, X. X.; Zhou, J.; Zhu, Q. Y.; Lei, Z. X.; Zhang, Y.; Dai, J. *Inorg. Chem.* **2008**, *47*, 8586–8588.
- (15) Vaqueiro, P. *Inorg. Chem.* **2008**, *47*, 20–22.
- (16) Wang, C.; Bu, X.; Zheng, N.; Feng, P. *Angew. Chem., Int. Ed.* **2002**, *41*, 1959–1961.
- (17) Manos, M. J.; Malliakas, C. D.; Kanatzidis, M. G. *Chem.—Eur. J.* **2007**, *13*, 51–58.

- (18) Wu, T.; Zuo, F.; Wang, L.; Bu, X.; Zheng, S.-T.; Ma, R.; Feng, P. *J. Am. Chem. Soc.* **2011**, *133*, 15886.
- (19) TOPAS, version 3; Bruker-AXS Inc.: Madison, WI, 1999.
- (20) Wendlandt, W. W.; Hecht, H. G. *Reflectance Spectroscopy*; Interscience Publishers: New York, 1966.
- (21) Bruker X8 APEX 2, version 1.0-8; Bruker AXS Inc.: Madison, WI, 2003.
- (22) Altomare, A.; Cascarano, G.; Giacovazzo, C.; Guagliardi, A.; Burla, M. C.; Polidori, G.; Camalli, M. *J. Appl. Crystallogr.* **1994**, *27*, 435.
- (23) Palatinus, L.; Chapuis, G. *J. Appl. Crystallogr.* **2007**, *40*, 786–790.
- (24) Watkin, D. J.; Prout, C. K.; Carruthers, J. R.; Betteridge, P. W. CRYSTALS; Chemical Crystallography Laboratory, University of Oxford: Oxford, U.K., 2006.
- (25) Cooper, R. I.; Gould, R. O.; Parsons, S.; Watkin, D. J. *J. Appl. Crystallogr.* **2002**, *35*, 168.
- (26) (a) Carpenter, J. D.; Hwu, S. J. *Inorg. Chem.* **1995**, *34*, 4647–4651. (b) Aleandri, L. E.; Ibers, J. A. *J. Solid State Chem.* **1989**, *79*, 107–111. (c) Messain, D.; Carré, D.; Laruelle, P. *Acta Crystallogr.* **1977**, *B33*, 2540–2542. (d) Tougait, O.; Ibers, J. A. *Inorg. Chem.* **2000**, *39*, 1790–1794.
- (27) Kemp, W. *Qualitative Organic Analysis: Spectrochemical Techniques*; McGraw-Hill book company, England, 1986.
- (28) Powell, A. V.; Lees, R. J. E.; Chippindale, A. M. *J. Phys. Chem. Solids* **2008**, *69*, 1000–1006.
- (29) (a) Osamura, K.; Murakami, Y.; Tomiie, Y. *J. Phys. Soc. Jpn.* **1966**, *21*, 1848. (b) Pfitzner, A.; Lutz, H. D. *J. Solid State Chem.* **1996**, *124*, 305–308.
- (30) Rigoult, J.; Rimsky, A. *Acta Crystallogr.* **1980**, *B36*, 916–918.
- (31) Hogg, J. H. C.; Sutherland, H. H.; Williams, D. J. *Acta Crystallogr.* **1973**, *B29*, 1590–1593.
- (32) Carré, D.; Guittard, M.; Adolphe, C. *Acta Crystallogr.* **1978**, *B34*, 3499–3501.
- (33) Walther, R.; Deiseroth, H. J. *Z. Kristallogr.* **1997**, *212*, 293.
- (34) (a) Deiseroth, H. J.; Reiner, C.; Schlosser, M.; Kienle, L. Z. *Anorg. Allg. Chem.* **2002**, *628*, 1641–1647. (b) Kienle, L.; Simon, A. *J. Solid State Chem.* **2002**, *167*, 214–225.
- (35) Merino, J. M.; Mahanty, S.; Leon, M.; Diaz, R.; Rueda, F.; Martin de Vidales, J. L. *Thin Solid Films* **2000**, *361–362*, 70–73.